Construction and Building Materials 329 (2022) 127118

Contents lists available at ScienceDirect

Construction and Building Materials

journal homepage: www.elsevier.com/locate/conbuildmat

Performance of sustainable concrete incorporating treated domestic wastewater, RCA, and fly ash

Abdelrahman Abushanab, Wael Alnahhal *

Department of Civil and Architectural Engineering, College of Engineering, Qatar University, Doha, Qatar

ARTICLE INFO

Keywords:
Treated wastewater
Recycled concrete aggregates
Fly ash
Durability
Morphological

ABSTRACT

This study evaluates the impact of using treated wastewater (TWW), recycled concrete aggregates (RCA), and fly ash (FA) on the mechanical, durability, and microstructural properties of concrete. A total of eight concrete mixes were manufactured and tested. Fresh mixing water and natural gabbro aggregates were completely replaced with TWW and RCA, respectively, whereas 20% of cement was substituted by FA. Test results revealed that TWW slightly reduced concrete mechanical properties by 6% to 12%, while it drastically reduced the chloride permeability by 77% in comparison with freshwater concrete. In addition, RCA decreased concrete compressive and flexural strengths by 21% and 10%, respectively, compared to natural aggregate concrete. Moreover, TWW concrete mixes with RCA had 16% to 42% lower porosity and chloride permeability than their counterparts with gabbro aggregates. Furthermore, concrete mixes with TWW, RCA, and FA exhibited the lowest chloride permeability among the investigated mixes. It was also shown that the interfacial transition zones between RCA and cement matrix were improved by replacing FA for 20% of cement. Analytically, aggregate and concrete morphological images and chemical composition were investigated to support the experimental results.

1. Introduction

At present, 10 billion tons of concrete are produced per year to sustain the unprecedented growth in population and urbanization over the world [1]. Such high demand puts pressure on the environment and long-term sustainability of concrete ingredients. The main ingredients being excessively consumed are coarse aggregates, which account for 60% to 75% of the total volume of concrete, and fresh water (FW) [1,2]. On a global scale, demand for FW and natural aggregates (NA) are as high as 2 [1] and 48.3 [3] billion tons per year, respectively. Meanwhile, demand for NA is predicted to rise by 40% by 2025 [4]. Moreover, the annual global consumption of ordinary Portland cement (OPC) exceeded 4.1 billion tons in 2018, accounting for 10% of the global CO_2 emissions [5]. This study accordingly investigated the feasibility of replacing FW, coarse NA, and OPC with recyclable materials in concrete manufacturing applications.

There are currently several alternatives to FW for concrete applications, one of which is treated domestic wastewater (TWW). Despite the common belief about the unsatisfactory impact of using TWW in concrete applications, a number of publications challenged this belief and acknowledged its viability in concrete [4,6–10]. Noruzman et al. [6] and Asadollahfardi et al. [7] found that concrete density and workability were slightly affected by TWW. Ahmed et al. [4] and Asadollahfardi et al. [7] revealed that TWW concrete recorded slightly lower compressive and flexural strengths than FW concrete at all ages. However, Arooj et al. [8] reported a 15% reduction in the compressive strength when FW was replaced with TWW. Shekarchi et al. [9] showed that the use of TWW decreased the electrical resistivity of concrete by 16%. Hassani et al. [11] and Saxena and Tembhurkar [12] found that the chloride permeability of TWW concrete specimens was remarkably higher than that of FW concrete. Abushanab and Alnahhal [1] and Asadollahfardi et al. [7] showed through scanning electron microscopy (SEM) analysis that concrete voids were increased with TWW.

Meanwhile, several recent attempts have focused on minimizing the rapid depletion of NA resources; one of these attempts relates to the use of recycled concrete aggregates (RCA), recycled from construction and demolition waste (CDW). In 2018, the global CDW annually disposed of was estimated at 3 billion tons [5]. Of this volume, 20,000 tons were daily generated in Qatar [3]. From a sustainability perspective, the use of RCA would minimize the CDW in landfills and reduce the economic and environmental impact of blasting, crushing, and transporting of NA [3]. Almost all studies have shown that the performance of recycled

* Corresponding author.
E-mail addresses: aa1104287@qu.edu.qa (A. Abushanab), wael.alnahhal@qu.edu.qa (W. Alnahhal).

https://doi.org/10.1016/j.conbuildmat.2022.127118
Received 21 September 2021; Received in revised form 11 February 2022; Accepted 9 March 2022
Available online 21 March 2022

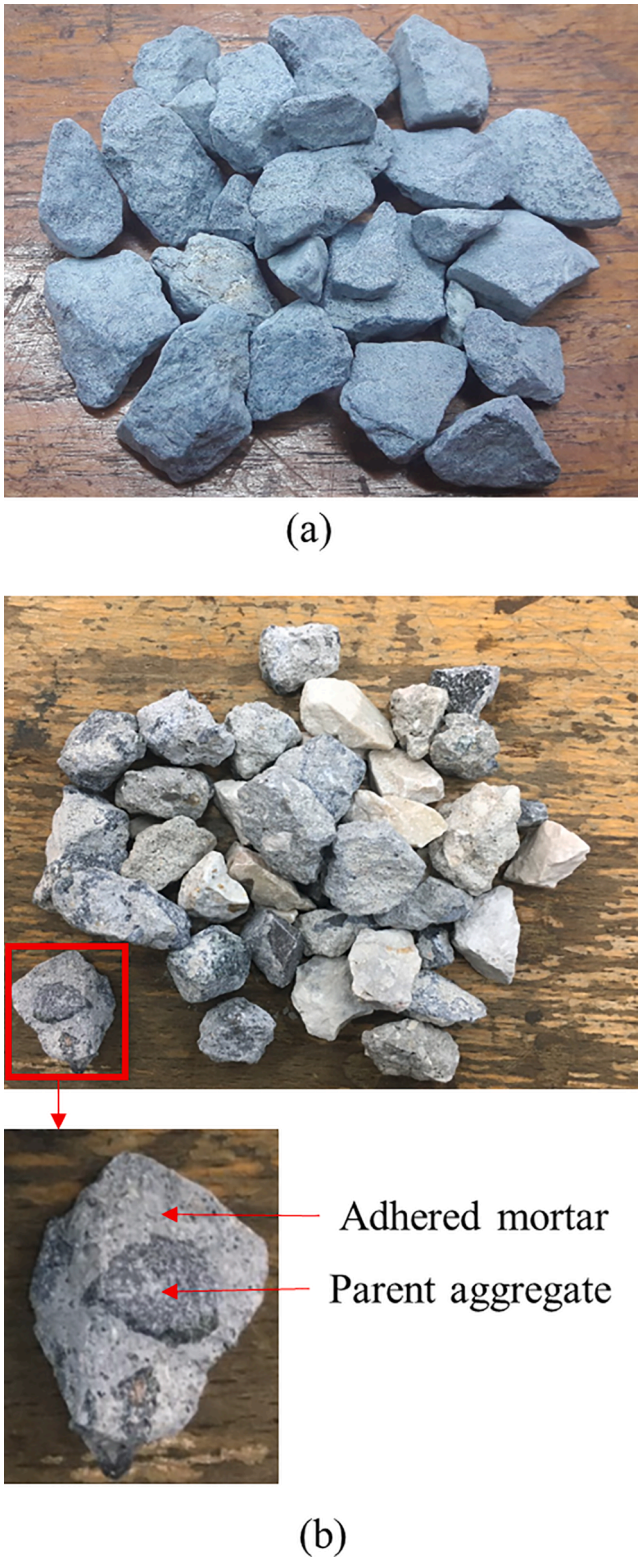

Fig. 1. The coarse aggregate used: (a) GA and (b) RCA.

aggregate concrete (RAC) was deteriorated by the weak interfacial transition zone (ITZ) between RCA and concrete matrix and RCAs' low density and high water absorption, crushing value, and porosity [13–16]. Huda and Alam [13] and Wang et al. [14] reported that RAC recorded 10% to 25% lower slump than NA concrete (NAC). Moreover, Abdulla [17] and Andreu and Miren [15] showed that RAC had a 5% to 9% lower density than NAC. Wang et al. [14] and Dimitriou et al. [16] noticed that RAC had 16% to 40% lower compressive strength than NAC. Alnahhal and Aljidda [2] and Ahmed et al. [4] found that the flexural strength of RAC was comparable with that of NAC, while Wang et al. [14] reported that the flexural strength of RAC exhibited a drop of 45%. As for the durability properties of RAC, Ahmed et al. [4] and de Brito et al. [18] noticed that RAC had a higher corrosion risk than NAC, attributable to the chloride ion penetration, electrical resistivity, and water permeability characteristics. Ali et al. [19] revealed that the pore volume of RAC was increased by raising the RCA replacement ratio. More recently, Ahmed et al. [4] investigated the mechanical and durability properties of concrete with TWW and 20% RCA. The authors found that RCA and TWW showed no significant effect on concrete durability.

Various techniques are currently being used to enhancing the performance of RAC. These techniques include: (i) removing of residual mortar by mechanical grinding, ultrasonic cleaning, and pre-soaking in acid [20], (ii) enhancing the ITZ layers by incorporating discrete fibers [19], and (iii) coating the surface of RCA with supplementary cementitious materials [19,21]. In particular, the use of fly ash (FA) improves the mechanical and durability properties of RAC by filling the voids in ITZ layers, producing additional calcium-silicate-hydrates (C–S–H) gel through the pozzolanic reaction between FA and $Ca(OH)_2$, and demobilizing the free chloride ions [19,21]. Lima et al. [22] and Kurda et al. [23] reported that the workability of RAC was considerably enhanced by a partial replacement of OPC with FA. Kou et al. [24] observed that the loss in the compressive strength of RAC could be mitigated by a 25% replacement of OPC with FA. Ali et al. [19] found that the water absorption and chloride resistance of RAC were enhanced with FA.

Even though researchers extensively investigated the effect of replacing FW with TWW, NA with RCA, and OPC with FA, very little data is available on the combined influence of TWW and RCA on concrete characteristics. Besides, none of the previous studies have addressed the characteristics of concrete simultaneously made with TWW, RCA, and FA. To this end, this study aimed at investigating the impact of using TWW, RCA, and FA simultaneously on the mechanical, durability, and microstructural characteristics of concrete.

2. Experimental program

2.1. Concrete constituents

2.1.1. Water

This study compared two types of mixing water, namely FW and TWW. The FW used complies with the requirements of drinking water as per the World Health Organization standards [25]. The TWW was obtained from Doha North Sewage Treatment Plant in Qatar. The chemical characteristics of FW and TWW were provided in Abushanab and Alnahhal [1]. The pH, residual chlorine, dissolved oxygen, BOD_5, and COD in FW and TWW were comparable. However, sulfate, total dissolved solids, chloride, phosphate, and zinc in TWW (490, 1690, 511, 9.19, 0.1051 mg/l, respectively) were significantly higher than those in FW (6, 93, 14.1, <0.03, 0.0046 mg/l, respectively). The characteristics of FW and TWW are within the acceptable limits of plain and reinforced concrete members as per ASTM C1602/C1602M-18 provisions [26].

2.1.2. Aggregates

This study investigated two types of coarse aggregates: gabbro (GA) and RCA. GA are coarse natural aggregates quarried from igneous rocks and characterized by a dark-grey color (Fig. 1(a)). GA is not available in Qatari local markets, and thus it is imported from Oman in large quantities to meet the domestic demand for the coarse aggregates. Its counterpart, RCA, are sourced from CDW and being produced in Qatar since 2009 [2]. The RCA used were derived from a 50 MPa compressive strength parent concrete. RCA are characterized by their rough and high porous surface texture (Fig. 1(b)). Furthermore, commercial wash sand was used in all concrete mixes as fine aggregates.

Table 1
Chemical composition of OPC and FA.

Chemical composition (% wt.*)	OPC	FA	OPC limit (ASTM C150/C150M – 20 [28])	FA limit (ASTM C618 – 19 [29])
Na_2O	–	0.06	–	–
SiO_2	15.84	55.97	Minimum 20	Minimum 50**
Al_2O_3	3.48	28.49	Maximum 6	–
MgO	2.5	1.57	Maximum 5	–
SO_3	2.8	0.51	Maximum 3	Maximum 5
P_2O_5	–	0.62	–	–
Cr_2O_3	0.05	0.04	–	–
CL	0.05	0.12	–	–
K_2O	0.47	1	–	–
CaO	68.91	2.74	–	Maximum 18
MnO	0.09	0.09	–	–
V_2O_5	0.05	0.04	–	–
Y_2O_3	–	0	–	–
TiO_2	0.28	1.95	–	–
ZrO_2	–	0.07	–	–
Fe_2O_3	4.8	6.63	Maximum 6	–
Nio	–	0.02	–	–
SrO	0.05	0.06	–	–

* wt. = weight
** For SiO_2, Fe_2O_3, and Al_2O_3 combined.

2.1.3. Cementitious materials

A general-purpose OPC CEM I 42.5R with a specific gravity of 3.15 was used in all concrete mixes. In addition, class F FA having a specific gravity of 2.23 was adopted at a replacement ratio of 20% by OPC weight to improve the durability characteristics of the mixes. The selection of the 20% FA replacement ratio is derived from a pilot study conducted by the authors in a previous study [1], where three FA replacement ratios (0%, 20%, and 35%) were experimentally and statistically investigated for concrete mechanical and durability properties, and the optimum FA ratio was found to be 20%. Furthermore, the chemical composition of OPC and FA were determined through X-ray fluorescence (XRF) analysis [27] and compared with ASTM C150/C150M – 20 [28] and ASTM C618 – 19 [29] provisions, respectively, as shown in Table 1. It could be seen that the calcium oxide (CaO) in FA is lower than that in OPC, indicating that the hydration rate in FA concrete mixes is lower than that in OPC mixes. Throughout the cement hydration process, C_3S ($3CaO{\cdot}SiO_2$) and C_2S ($2CaO{\cdot}SiO_2$) react with water to form calcium hydroxide and calcium silicate hydrate gel. However, with the absence of enough CaO, FA concrete mixes would experience lower early compressive strength than 100% OPC concrete mixes. By contrast, the silica content in FA was much higher compared to that in OPC, signifying the secondary pozzolanic reaction of FA concrete mixes, which increases the strength and durability characteristics at later ages. The properties of the OPC and FA were within the acceptable limits of ASTM C150/C150M-20 [28] and ASTM C618 – 19 [29] specifications, respectively.

2.2. Concrete mixtures composition

Eight concrete mixes were produced by replacing FW with TWW, GA with RCA, and 20% of OPC with FA. The replacements of TWW and FA were by weight of FW and OPC, respectively, whereas the replacement of GA with RCA was by volume. Different replacement methods for FA and RCA were used for the purpose of achieving a higher ratio of fresh mortar to coarse aggregate and therefore improving concrete properties. Knowing that FA has lower specific gravity than OPC, the 20% of OPC was replaced with FA using the mass replacement method to increase the ratio of fresh mortar to coarse aggregates and consequently enhance concrete workability. In addition, RCA have lower specific gravity than GA. Therefore, GA were replaced with RCA by volume to increase the ratio of binders to coarse aggregates and, in turn, improve concrete workability and compressive strength. Furthermore, according to Eddy et al. [30], domestic wastewater has a similar density to FW. Thus, the mass replacement method was used to replace FW with TWW. Trial mixes with different water/binder ratios were produced to achieve a 50 MPa target compressive strength at 28 days. All concrete mixes were produced with a constant amount of superplasticizer to study the influence of the tested parameters on concrete workability. The composition of all concrete mixes are provided in Table 2. The designation of concrete mixes is as follows: the first letter represents the mixing water type (F and T for FW and TWW, respectively). The second letter refers to the coarse aggregate used (G and R for GA and RCA, respectively). The last letter identifies the cementitious material type, where "O" indicates that the mix is completely made with OPC, and "F" indicates that 20% of OPC was replaced with FA.

Table 2
Concrete mix composition.

Mix	Unit weight (kg/m^3)							
	FW	TWW	GA	RCA	Sand	OPC	FA	SP
F-G-O	156.4	0	1075.5	0	708.1	349.2	0	0.7
T-G-O	0	156.4	1075.5	0	708.1	349.2	0	0.7
F-R-O	156.4	0	0	942.4	708.1	349.2	0	0.7
T-R-O	0	156.4	0	942.4	708.1	349.2	0	0.7
F-G-F	156.4	0	1075.5	0	708.1	279.3	69.8	0.7
T-G-F	0	156.4	1075.5	0	708.1	279.3	69.8	0.7
F-R-F	156.4	0	0	942.4	708.1	279.3	69.8	0.7
T-R-F	0	156.4	0	942.4	708.1	279.3	69.8	0.7

Note: SP = superplasticizer.

Table 3
Relationships between corrosion risks, resistivity, and charge transferred as per AASHTO TP 95 [40] and ASTM C1202-19 [42], respectively.

Resistivity (kΩ•cm)	Corrosion Risk	Charge transferred (Coulomb)
<12	High	>4000
12–21	Moderate	2000–4000
21–37	Low	1000–2000
37–254	Very low	100–1000
>254	Negligible	<100

2.3. Aggregate and concrete tests

2.3.1. Aggregate tests

Aggregate physical properties, including specific gravity (ASTM C127–15 [31]), water absorption (ASTM C127–15 [31]), abrasion resistance (ASTM C131–20 [32]), elongation and flakiness indices (BSI-1998 [33]), and soundness (ASTM C88–18 [34]), were measured. In addition, the gradation analysis for GA, RCA, and wash sand was performed in accordance with ASTM C33/C33M-18 standards [35].

2.3.2. Concrete mechanical properties

Concrete fresh slump (ASTM C143/C143M-15a [36]) and density (ASTM C138/C138M-17a [37]) were measured instantly after mixing. Moreover, the compressive strength was evaluated using three 100 × 200 mm cylinders from each mix as per ASTM C39/C39M-20 provisions [38]. The compression tests were performed at 7, 28, and 90 days at a 0.2 MPa/sec loading rate. Furthermore, the flexural tensile strength tests were conducted on three 100 × 100 × 500 mm prisms from each mix according to ASTM C78/C78M-18 provisions [39]. The flexural tests were performed at 28 and 90 days at a 0.58 kN/sec loading rate.

2.3.3. Concrete durability tests

The electrical resistivity of concrete was evaluated following AASHTO TP 95 standards [40]. Three 100 × 200 mm cylinders from each mix were tested after 7, 28, and 90 days of curing. Table 3 illustrates the relationship between the corrosion risks and concrete electrical resistivity. In addition, concrete porosity tests were performed at

Table 4
Physical properties of the coarse aggregates and sand.

Property	GA	RCA	Wash sand	QCS 14 limit [44]
Bulk Specific Gravity (Dry)	2.89	2.47	2.62	—
Bulk Specific Gravity (SSD[a])	2.91	2.55	2.63	—
Bulk Specific Gravity (APP[b])	2.95	2.70	2.65	—
Water Absorption (%)	0.72	3.51	0.6	2[c] 3[d] 2.3[e]
Abrasion Loss (%)	8.9	17.6	—	30
Elongation Index (%)	24	8	—	35
Flakiness Index (%)	6.9	5.2	—	35
Soundness (%)	2.2	12.6	10.3	15

Note:.
a = SSD for saturated surface dry.
b = APP for apparent.
c = maximum for natural aggregates.
d = maximum for RCA.
e = maximum for fine aggregates.

28 and 90 days using two 100 × 50 mm cylinders from each mix according to ASTM C1754/C1754M-12 guidelines [41]. The cylinders were sliced from 100 × 200 mm cylinders. The specimens were oven-dried at 38 °C for 24 h and weighed. This process was repeated until a 0.5% difference in weight was obtained. Thereafter, the cylinders were immersed in water for 30 min and weighed. Finally, concrete porosity was calculated using Eq. (1):.

$$Porosity = \left[1 - \left(\frac{K \times (A - B)}{\rho_w \times D^2 \times L}\right)\right] \times 100 \quad (1)$$

where K is a constant (1273240 mm^3kg/m^3g), A and B are the specimen's dry and submerged weight (g), respectively, D and L are the specimen's diameter and height (mm), respectively, and ρ_w is the density of water (kg/m^3). Moreover, the rapid chloride penetration test (RCPT) was done on two 100 × 50 mm cylinders for each mix after 28 and 90 days of curing as per ASTM C1202-19 standards [42]. Concrete cylinders of 100 × 200 mm were first sliced into 100 × 50 mm cylinders and then oven-dried at 50 °C for three days. Afterward, the sliced specimens were epoxy coated on their outer circumferences, vacuumed in a desiccator for 3 h, and then immersed in deaerated water for 18 h. Subsequently, each sliced specimen was mounted between two polyacrylic boxes under a 60 V potential difference for 6 h. The first box was filled with a 0.3 N concentrated sodium hydroxide (NaOH) solution, whilst the second box was filled with a 3% concentrated sodium chloride (NaCl) solution. The number of Coulombs transferred was recorded as per the time duration mentioned in ASTM C1202-19 standards [42] according to Eq. (2):.

$$Q = 900(I_0 + 2I_{30} + 2I_{60} + \cdots + 2I_{300} + 2I_{330} + I_{360}) \quad (2)$$

where I_0, I_{30}, etc are the current applied at time = 0, 30, etc minutes. Table 3 illustrates the relationship between the corrosion risks and Coulomb charges.

2.3.4. Microstructural tests

The microstructural formation of concrete and coarse aggregates was tested using SEM images according to ASTM C1723-16 standards [43]. The SEM images were taken on fractured surface specimens using a NOVA NANOSEM 450 instrument. Moreover, the mineralogy of cementitious matrices and coarse aggregates was determined by the X-ray diffraction (XRD) analysis using an S2 Puma Bruker ® instrument.

3. Results and discussion

3.1. Aggregate gradation and physio-chemical properties

The physical properties of coarse and fine aggregates along with the requirements specified in Qatar Construction Specifications (QCS-14) [44] are demonstrated in Table 4. It could be seen from the table that the measured properties of both types of aggregates were within the permissible limits of QCS-14 [44], except for the water absorption of RCA, which exceeded the limit by 17% due to the adhered mortar and porous nature of RCA. Moreover, RCA recorded about 15% lower specific gravity, 5 times higher water absorption, and 2 times higher abrasion loss than GA. In addition, due to the significant differences in the specific gravity and water absorption between the two types of aggregates, GA and RCA were soaked in water for 24 h before mixing to achieve a saturated surface dry (SSD) condition for both aggregate types. Having the coarse aggregates in the SSD condition ensures uniformity in aggregates' pores and water absorption. Furthermore, the gradation curves for fine and coarse aggregates are plotted in Fig. 2. As shown in the figure, both types of aggregates were within the limits recommended by ASTM C33/C33M-18 standards [35].

3.2. Aggregate microstructural and mineralogy analysis

The SEM images of GA and RCA at different magnifications are shown in Fig. 3(a)–(d). It could be noticed from the SEM images that GA

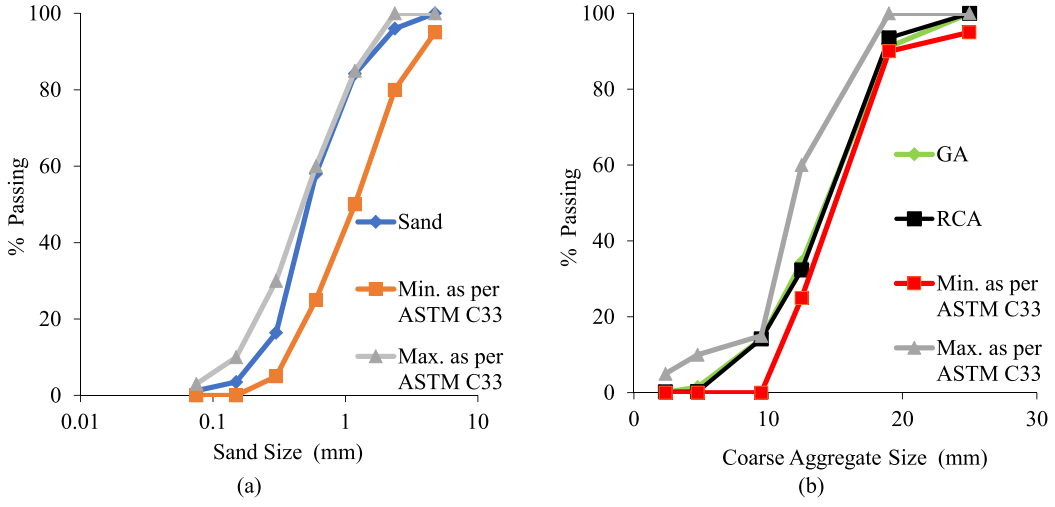

Fig. 2. Sieve analysis for sand and coarse aggregate used.

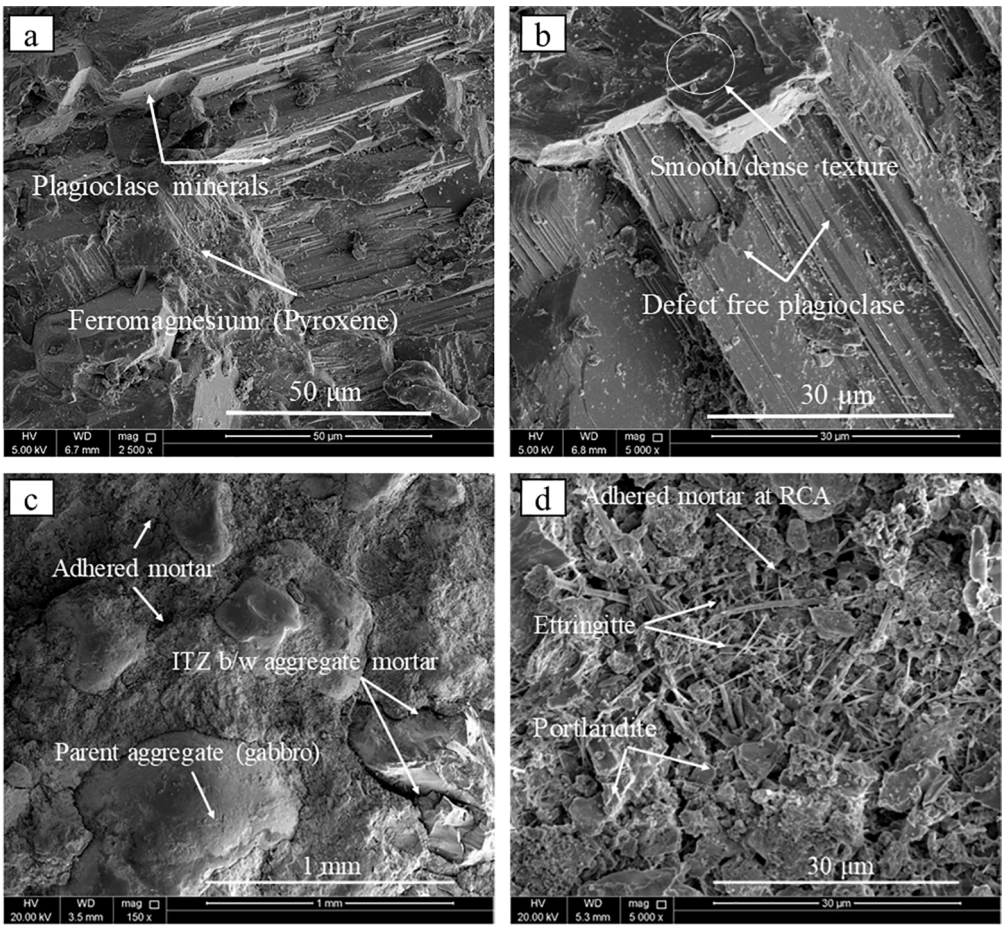

Fig. 3. Coarse aggregate SEM images for: (a, b) GA and (c, d) RCA.

have a denser and more homogeneous microstructure and lesser surface porosity than RCA. It was also observed that GA are rich in plagioclase-mineral crystals and ferromagnesium (pyroxene) minerals. The dense microstructure of GA could explain why GA showed lower water absorption and Los Angeles abrasion loss than RCA (see Table 4). The presence of parent concrete's impurities such as OPC mortar, ettringite needles, and portlandite crystals can also been seen in the SEM images of RCA. The presence of these impurities on RCA surface deteriorates the water absorption and Los Angeles abrasion resistance of RCA (see Table 4). These impurities also create additional and weak ITZ layers in the matrix, which further increases the water absorption and deteriorates the durability properties of concrete.

The mineralogical phases of GA and RCA are shown in Fig. 4(a) and (b). It could be seen from the figures that GA are composed of alumino-calcium-silicates ($CaAl_2Si_2O_8$) (i.e., named anorthite in Fig. 4(a)), ferromagnesium, fersilitcite, magnetite, and iron oxide. The higher abrasion resistance of GA in comparison with RCA can be linked to the presence of fersilitcite, magnetite, and iron oxide. On the other hand, the main impurities found in RCA were sodium nitrate ($NaNO_3$), portlandite ($Ca(OH)_2$), carbon dioxide (CO_2), calcium hydroxide cobalt oxide ($(CaOH)_{1.14}CoO_2$), anorthite ($CaAl_2Si_2O_8$), and dipotassium sulfates (K_2SO_2). These impurities create additional ITZ layers between RCA and cement matrix, which further increase the water absorption and deteriorate the durability properties of RAC. Furthermore, the presence of anorthite impurity in RCA suggests that the RCA used were originally GA.

3.3. Concrete fresh properties

As shown in Table 5, replacing FW with TWW in mixes T-G-O, T-R-O, T-G-F, and T-R-F showed no significant difference in the fresh slump and density results. This is mostly attributed to the close total suspended solids in both TWW and FW. Despite that aggregates' tests showed that GA have higher density and denser microstructure than RCA, it was revealed that RAC mixes F-R-O, T-R-O, F-R-F, and T-R-F recorded almost similar fresh properties to those made with GA. That was because both GA and RCA were in SSD condition before mixing, of which the RCA and adhered mortar pores were filled with water, achieving approximately similar solid weights and water absorption to GA. Moreover, it could be observed that the substitution of 20% of OPC by FA in mixes F-G-F, T-G-F, F-R-F, and T-R-F resulted in a 53% to 59% higher slump than those made completely with OPC. This is attributed to the dilution effect, resulting from the replacement of 20% OPC with FA. The dilution effect, in turn, increased the water-to-cement ratio and thus increased concrete flow. The improved workability of FA concrete mixes could also be attributed to the small-spherical morphology particles of the FA, which reduced the friction with other concrete constituents. An SEM image showing the spherical particles of the FA is shown in Fig. 5. Furthermore, substituting 20% of OPC by FA did not affect concrete density because of the low FA quantity used. The obtained results are consistent with Abushanab et al. [5], Noruzman et al. [6], and Kurda et al. [23].

3.4. Concrete mechanical and durability properties

The hardened mechanical and durability characteristics of the eight concrete mixes were tested at 7, 28, and 90 days. As expected, the results demonstrate that all concrete mixes achieved better mechanical and durability results at higher curing periods, regardless of the type of mixing water, coarse aggregates, and cementitious material. That is fundamentally linked to the OPC hydration with time and the secondary

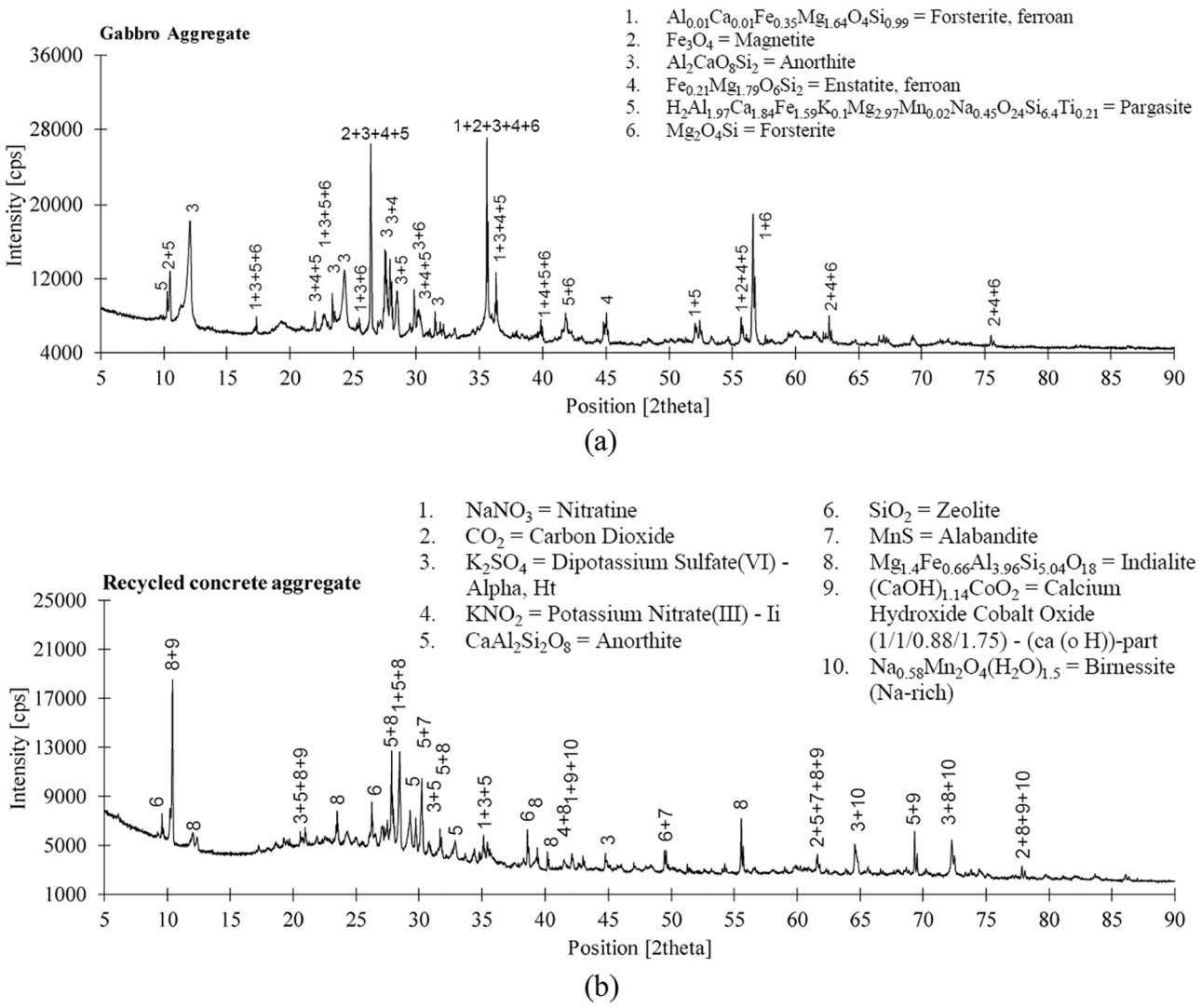

Fig. 4. XRD analysis for: (a) GA and (b) RCA.

Table 5
Concrete fresh slump and density results.

Mix	Slump (mm)	Density (kg/m^3)
F-G-O	86	2473
T-G-O	91	2448
F-R-O	82	2389
T-R-O	89	2391
F-G-F	135	2465
T-G-F	145	2506
F-R-F	130	2349
T-R-F	136	2354

reaction of FA with $Ca(OH)_2$, which consequently enhanced the ITZ layers. In addition, all concrete mixes had "low" and "very low" corrosion risk at 90 days as per AASHTO TP 95 [40] and ASTM C1202-19 [42] specifications (see Table 3). The following subsections provide details of concrete mechanical and durability test results:.

3.4.1. Compressive strength

The average compressive strength results of the eight concrete mixes at 7, 28, and 90 days are demonstrated in Fig. 6. It was observed that replacing FW with TWW slightly decreased the compressive strength of concrete. As shown in Fig. 6(a), specimen T-G-O recorded 11.7%, 6.1%,

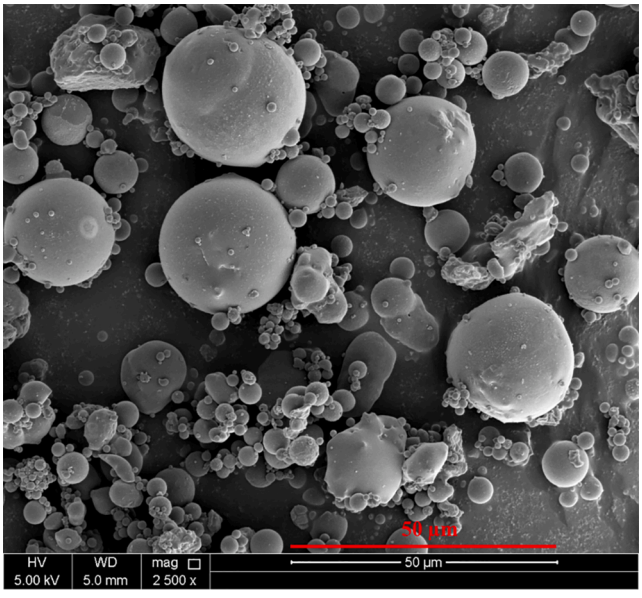

Fig. 5. An SEM image for the spherical particles of the FA.

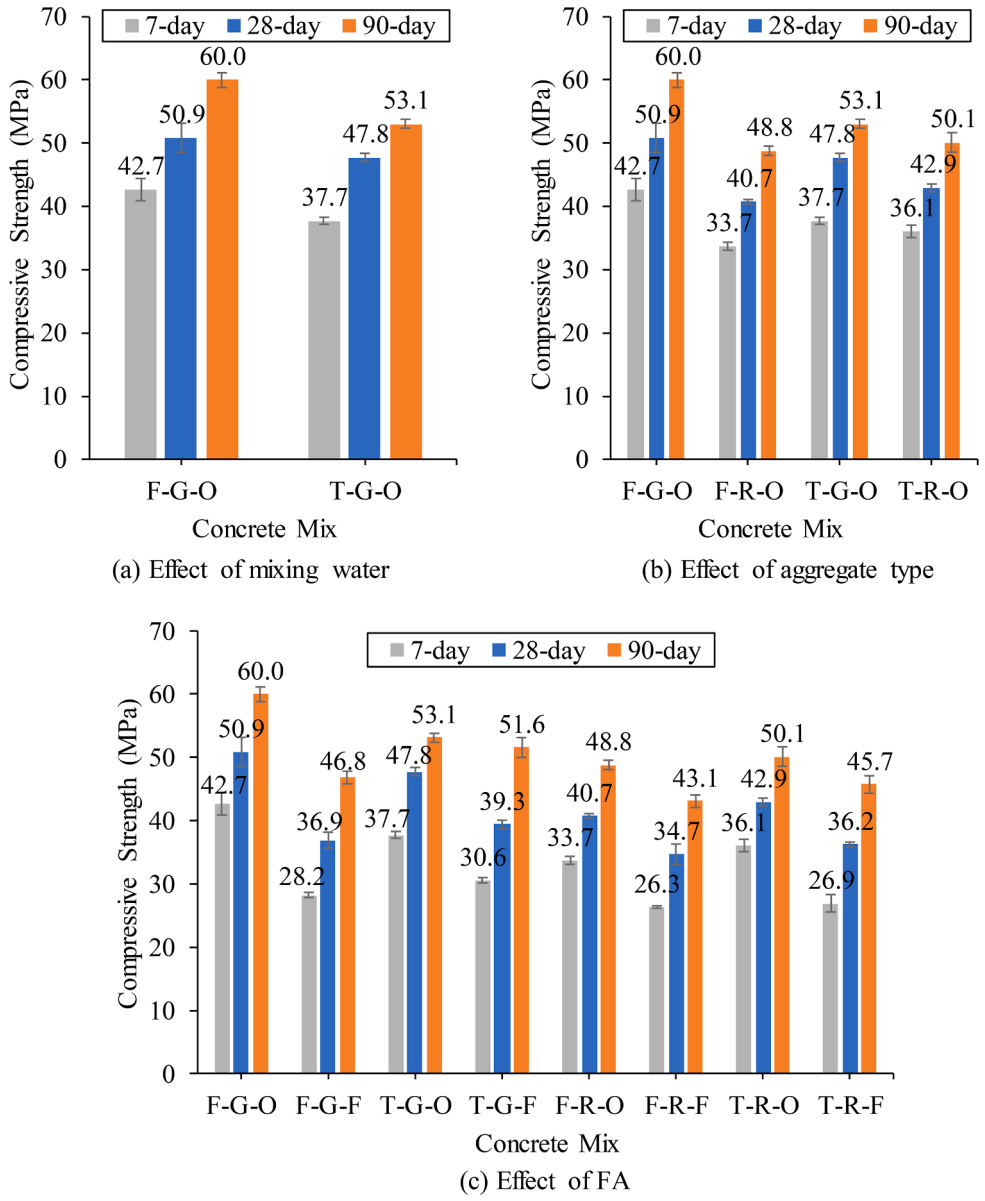

Fig. 6. Compressive strength of concrete mixes at different curing periods.

and 11.5% lower compressive strength than specimen F-G-O at 7, 28, and 90 days, respectively. This reduction is mainly due to the high phosphate, zinc, and suspended solids in TWW, which delayed the OPC hydration process and weakened the ITZ layers in concrete. In particular, OPC particles react with phosphate salts and produce a layer of Ca-phosphate. This layer, in turn, isolates water from OPC particles and consequently delays the OPC hydration process [45]. Moreover, the hydration of OPC in the presence of zinc is also delayed due to the formation of an amorphous layer of $Zn(OH)_2$, which subsequently transformed into $CaZn_2(OH)_6{\cdot}2H_2O$. The chemical reactions describing the influence of zinc on the hydration of C_3S are presented in Eqs. (3) to (5). Such reactions delay the formation of C_3S hydration products [46].

$$Zn^{2+} + 2OH^- \rightarrow Zn(OH)_2 \quad (3)$$

$$Zn(OH)_2 + 2OH^- \rightarrow 2H_2O + ZnO_2^{2-} \quad (4)$$

$$2ZnO_2^{-2} + C_3S/O - Ca^{2+} + 6H_2O \rightarrow C_3S/O - CaZn_2(OH)_6 \bullet 2H_2O + 2OH^- \quad (5)$$

In addition, the presence of suspended solids in TWW increased concrete voids and weakened the ITZ layers in concrete and thus decreased the compressive strength of concrete. Similarly, Arooj et al. [8] reported that TWW concrete exhibited 11% to 15% lower compressive strength than FW concrete.

Moreover, it was found that RAC specimens reported lower compressive strength than GA concrete specimens (Fig. 6(b)). For instance, the compressive strength of specimens F-R-O and T-R-O was decreased by 21.1% and 4.2% at 7 days, 20% and 10.3% at 28 days, and 18.7% and 5.6% at 90 days compared to their counterparts with GA. The drop in the compressive strength of RAC specimens is attributed to the additional ITZ layers in RAC, which affected concrete internal cracks and pores and, in turn, increased the microcracks and accelerated the bond failure between RCA and concrete matrix. The drop in the compressive strength of RAC might also be linked to the low density of RCA compared to GA. Moreover, the results showed that the rate of reduction of specimen F-R-O decreased as the curing period increased, owing to the secondary reaction between water and un-hydrated cement particles from parent concrete. The results are in conformance with Dimitriou et al. [16] and Ali et al. [19] experimental results. Furthermore, in agreement with Ahmed et al. [4], no severe drop was detected on the compressive strength of specimen T-R-O compared to F-R-O. As

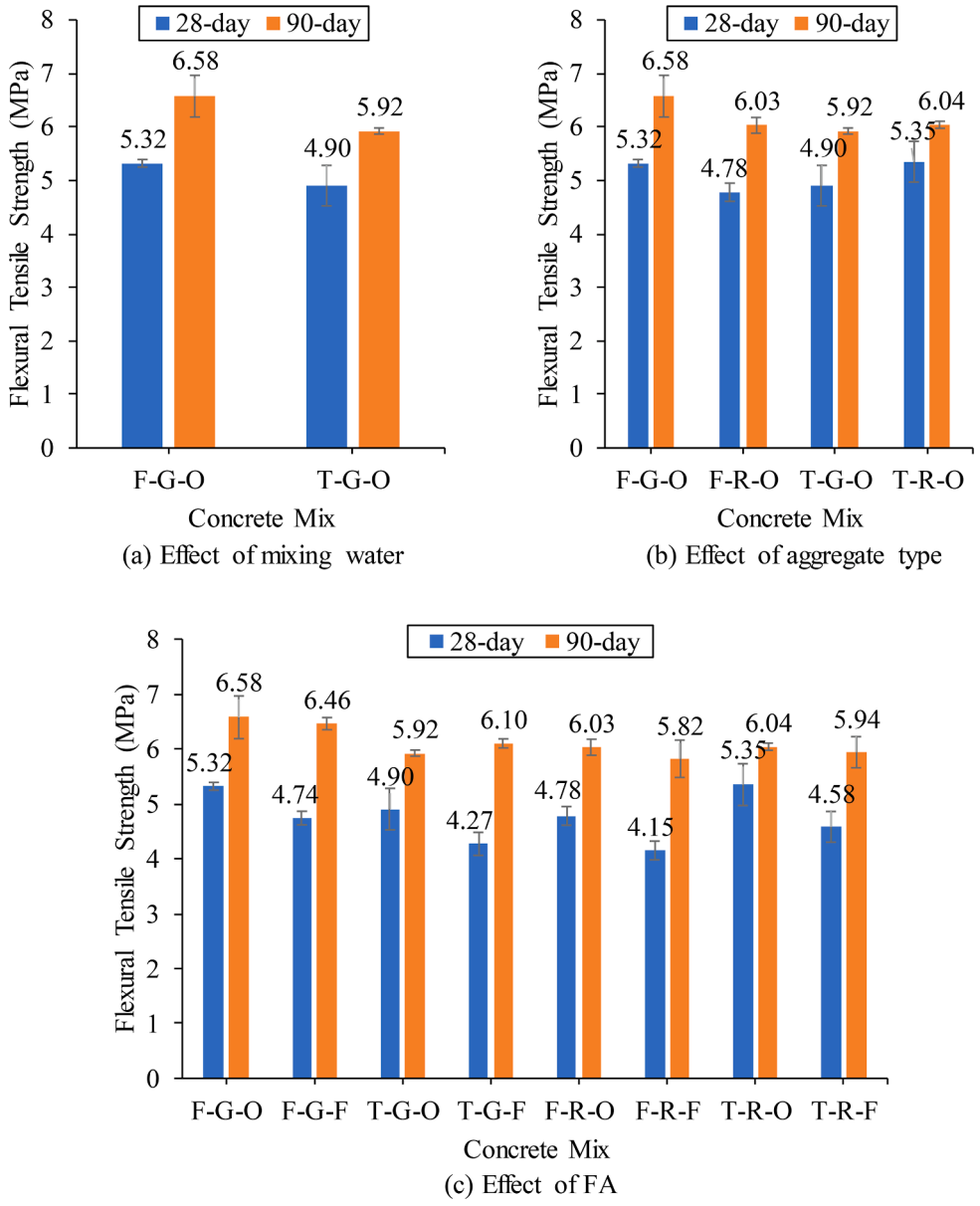

Fig. 7. Flexural tensile strength of concrete mixes at different curing periods.

presented in aggregate XRD analysis (see Fig. 4(b)), RCA are composed of high intensities of calcium, which reacted with sulfate in TWW and generated calcium monosulphoaluminate hydrate (C_4ASH_{12}). Calcium monosulphoaluminate, in turn, enhanced the ITZ layers in concrete matrix and consequently improved concrete compressive strength [47].

Regarding the influence of FA on the compressive strength of concrete, Fig. 6(c) shows that the incorporation of 20% FA in specimens F-G-F, T-G-F, F-R-F, and T-R-F decreased the compressive strength by 33.9%, 18.8%, 21.9%, and 25.5% at 7 days, respectively, compared to their counterparts with no FA. However, the rate of reduction decreased to 27.5%, 17.8%, 14.7%, 15.6% at 28 days and 22%, 2.82%, 11.7%, and 8.8% at 90 days, respectively, compared to their counterparts with no FA. That was expected because the pozzolanic reaction between FA and $Ca(OH)_2$ to produce C–S–H gel occurs at later concrete ages. The results also demonstrate that mix T-R-F achieved 6% higher compressive strength than mix F-R-F at 90 days. Moreover, the net gain in the compressive strength of mix T-R-F at 28 days was 11.8%, 21.5%, and 8.2% higher than mixes F-G-F, T-G-F, and F-R-F, respectively. The outperformance of mix T-R-F in the compressive strength gain is attributed to the formation of monosulphoaluminate hydrate and C–S–H gel, which filled the pores and cracks induced by the suspended particles of TWW and adhered mortar of RCA. The enhancement also related to the $Ca(OH)_2$ available on the surface of RCA, which improved the pozzolanic reaction of FA and resulted in more densified microstructure. This reveals that FA has a more influential effect on mix T-R-F than other mixes. Similar observations were also reported by Ali et al. [19] and Kurad et al. [48].

3.4.2. *Flexural tensile strength*

As could be seen from Fig. 7, the flexural tensile strength results of all concrete mixes showed a similar trend to the compressive strength results. For instance, prism T-G-O achieved 7.9% and 10% lower flexural strength than F-G-O at 28 and 90 days (Fig. 7(a)), respectively, owing to the high concentration of phosphate, zinc, and suspended solids in TWW, which delayed the OPC hydration process, weakened the ITZ layers, and increased concrete internal cracks.

Moreover, Fig. 7(b) shows that the use of RCA in prism F-R-O decreased the flexural strength by 10.2% and 8.4% at 28 and 90 days,

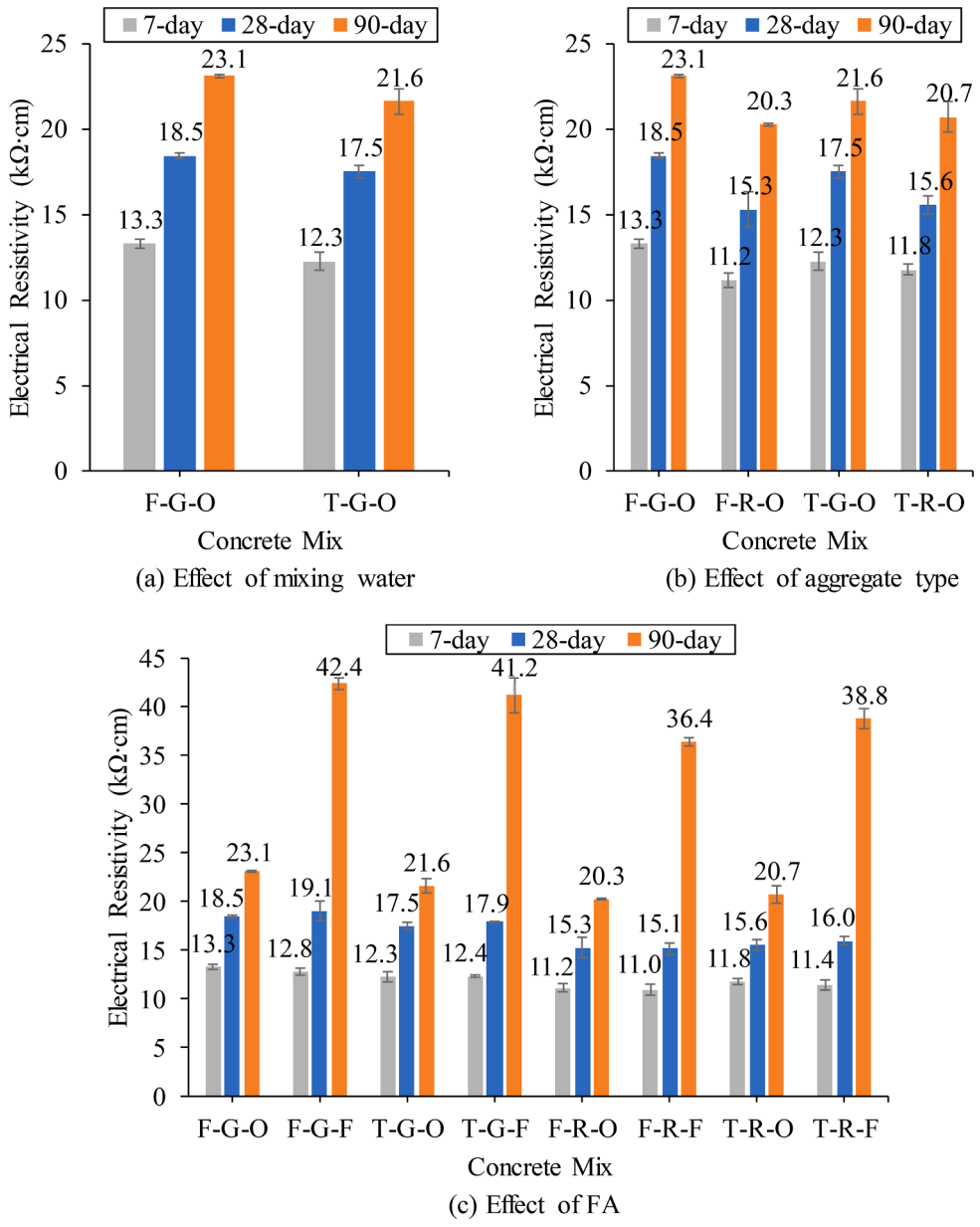

Fig. 8. Concrete electrical resistivity results at different curing periods.

respectively. This is fundamentally attributed to the adhered mortar on RCA, which increased concrete cracks and voids. On the other hand, it was observed that TWW-RAC prism T-R-O exhibited 9.2% and 2% higher flexural strength than TWW-GA prism T-G-O at 28 and 90 days, respectively, attributable to the formation of calcium monosulphoaluminate hydrate, which improved the cohesion of the ITZ layers between the old and new mortars.

Furthermore, incorporating 20% FA in specimens F-G-F, T-G-F, F-R-F, and T-R-F decreased the flexural strength by 10.9%, 12.9%, 13.2%, and 14.4% at 28 days (Fig. 7(c)), respectively. This could be ascribed to the reduced cohesion between aggregates and cement matrix, as the amount of OPC was decreased. It could also be noticed that at 90 days, FA prisms made with TWW and/or RCA recorded approximately similar flexural strength to their companions with 100% OPC due to the pozzolanic reaction of FA, which generated more C–S–H gel and consequently densified the concrete matrix. In addition, the proposed mix T-R-F exhibited 10.4% higher flexural strength at 28 days than its counterpart mix with fresh water (F-R-F). The enhancement of mix T-R-F over mix F-R-F is attributed to the formation of monosulphoaluminate hydrate and C–S–H gel, which improved the ITZ layers. The results are in conformance with Asadollahfardi et al. [7] and Ali et al. [19].

3.4.3. *Electrical resistivity*

The variations in concrete electrical resistivity with respect to TWW, RCA, and FA are presented in Fig. 8. Electrical resistivity results recorded no significant loss when FW was replaced with TWW. As shown in Fig. 8(a), specimen T-G-O recorded 7.5%, 5.4%, and 6.4% lower resistivity than specimen F-G-O at 7, 28, and 90 days than F-G-O, respectively. The slight reduction is mainly caused by the suspended solids of TWW, which increased concrete pores and accelerated the electrical current movement. Moreover, TWW is composed of a higher amount of iron than FW, which, in turn, accelerated the movement of electrical currents.

By observing the resistivity of RAC specimens in Fig. 8(b), it could be recognized that the electrical resistivity of specimens F-R-O and T-R-O had an average decrease of 15.1% and 6.4% compared to their respective with GA, respectively. This is ascribed to the adhered mortar on RCA, which weakened the ITZ layer between aggregates and cement

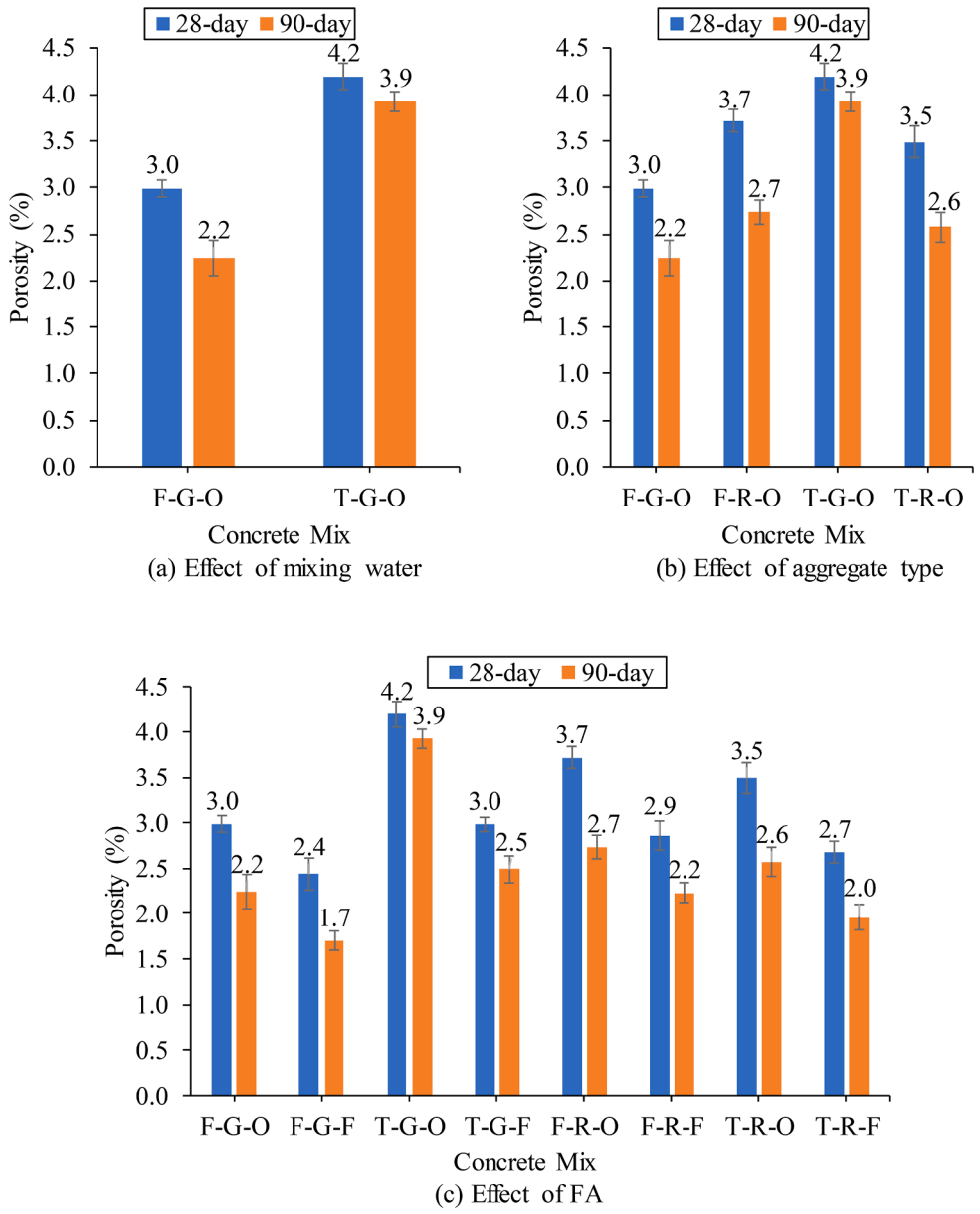

Fig. 9. Porosity of concrete mixes at different curing periods.

matrix and thus accelerated the electron movement. Complying with the hardened mechanical properties of concrete, TWW-RAC specimens showed a lower rate of reduction than the FW-RAC specimens, owing to the calcium monosulphoaluminate hydrate, which improved the ITZ layers between the old and new mortars.

On the other hand, the electrical resistivity results of FA concrete mixes reinforce the general belief about the pozzolanic reaction between FA and $Ca(OH)_2$ to densify the cement matrix at later ages by the C–S–H gel. At 7 days, the FA concrete specimens F-G-F, T-G-F-, F-R-F, and T-R-F recorded slightly lower resistivity than their counterparts made entirely with OPC. However, at 28 and 90 days, FA concrete specimens reported significantly higher resistivity than other mixes, regardless of mixing water and aggregate types (Fig. 8(c)). Regarding the proposed interaction among TWW, RCA, and FA, it was observed that mix T-R-F achieved 6.6% higher resistivity than mix F-R-O at 90 days. In addition, the resistivity of mix T-R-F at 90 days outweighed the resistivity of the reference mix (F-G-O) by 68%, owing to the monosulphoaluminate hydrate and C–S–H gel formed in mix T-R-F. These observations are in agreement with Abushanab and Alnahhal [1], Shekarchi et al. [9], and Andreu and Miren [15].

3.4.4. Porosity

The results illustrated in Fig. 9(a) reveal that the use of TWW for concrete mixing significantly affected the porosity of concrete. For instance, specimen T-G-O recorded 40% and 77.3% higher porosity than specimen F-G-O at 28 and 90 days, respectively. Furthermore, the rate of decrease in TWW concrete porosity with time was lower than that made with FW. After 90 days of curing, the porosity of specimen F-G-O was decreased by 26.7%, whereas specimen T-G-O had a reduction of only 7.1% compared to those at 28 days. This is ascribed to the high concentration of zinc, phosphate, and suspended solids in TWW, which alerted the OPC hydration and weakened the ITZ layers in concrete.

The results also indicate that the substitution of GA with RCA in specimens F-R-O and T-R-O increased concrete porosity by 23.3% and 22.7% at 28 and 90 days, respectively, compared to F-G-O (Fig. 9(b)). This could be ascribed to the adhered-porous mortar on RCA, which created more voids and consequently weakened the ITZ layer between old and new mortars. In addition, it was observed that the substitution of

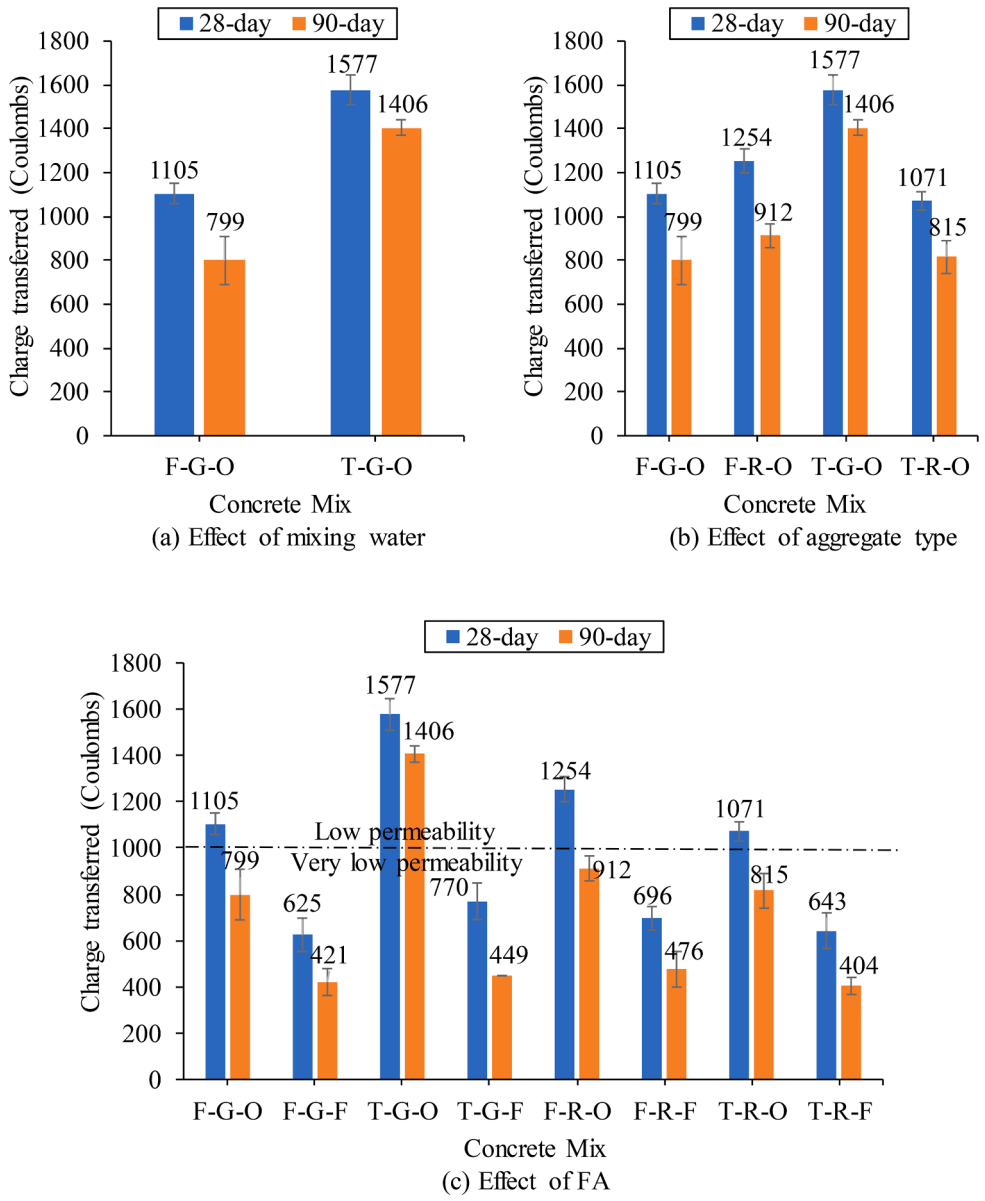

Fig. 10. Chloride permeability of concrete mixes at different curing periods.

GA by RCA in specimen T-R-O resulted in 16.7% and 33.3% lower porosity than T-G-O at 28 and 90 days, respectively. This has occurred due to the formation of calcium monosulphoaluminate hydrate, which enhanced concrete microstructure. This might explain why specimen T-R-O reported slightly higher compressive strength than F-R-O. Regarding the influence of increasing curing period on RAC porosity, it was observed that RCA had no effect on porosity reduction with time, as specimens F-R-O and T-R-O exhibited similar porosity reduction at 90 days compared to specimens F-G-O and T-G-O.

In conformance with the resistivity results, Fig. 9(c) shows that the incorporation of 20% FA greatly decreased concrete porosity, regardless of mixing water and aggregate types. Specimens F-G-F, T-G-F, F-R-F, and T-R-F recorded an enhancement in concrete porosity of 20%, 28.6%, 21.6%, and 22.9% at 28 days and 22.7%, 35.9%, 18.5%, and 23.1% at 90 days, respectively, compared to their counterparts without FA. This is explained by the pozzolanic reaction between FA and $Ca(OH)_2$ to produce C–S–H gel and consequently densify concrete microstructure. The results also showed that specimen T-R-F reported about 10% lower porosity than the control specimen (F-G-O). As well, specimen T-R-F exhibited 6% to 20% lower porosity than specimens T-G-F, F-R-F, and T-R-F. Moreover, the porosity reduction of specimen T-R-F with time was 7.3% and 56.1% higher than that of specimens F-R-F and T-G-F, respectively. This is attributed to the combined effects of the monosulphoaluminate hydrate, small-size particles and pozzolanic reaction of FA, and pozzolanic reaction between residual $Ca(OH)_2$ on RCA and FA, which have effectively densified the mix's microstructure. The obtained results agree with Abushanab and Alnahhal [1] and Lima et al. [22].

3.4.5. *Chloride permeability*

In conformance with the porosity and resistivity results, Fig. 10(a) demonstrates that the substitution of FW with TWW has substantially increased concrete chloride permeability. This could be seen in specimen T-G-O, where it recorded 42.7% and 76% higher Coulomb charges than specimen F-G-O at 28 and 90 days, respectively. This is mainly ascribed to the presence of chloride ions in TWW, which accelerated the movement of Coulomb charges. Moreover, because phosphate and zinc in TWW delay the cement hydration process, the rate of decrease in the chloride permeability of specimen T-G-O was 61% lower than that of F-G-O at 90 days.

Furthermore, the results showed that the substitution of GA with

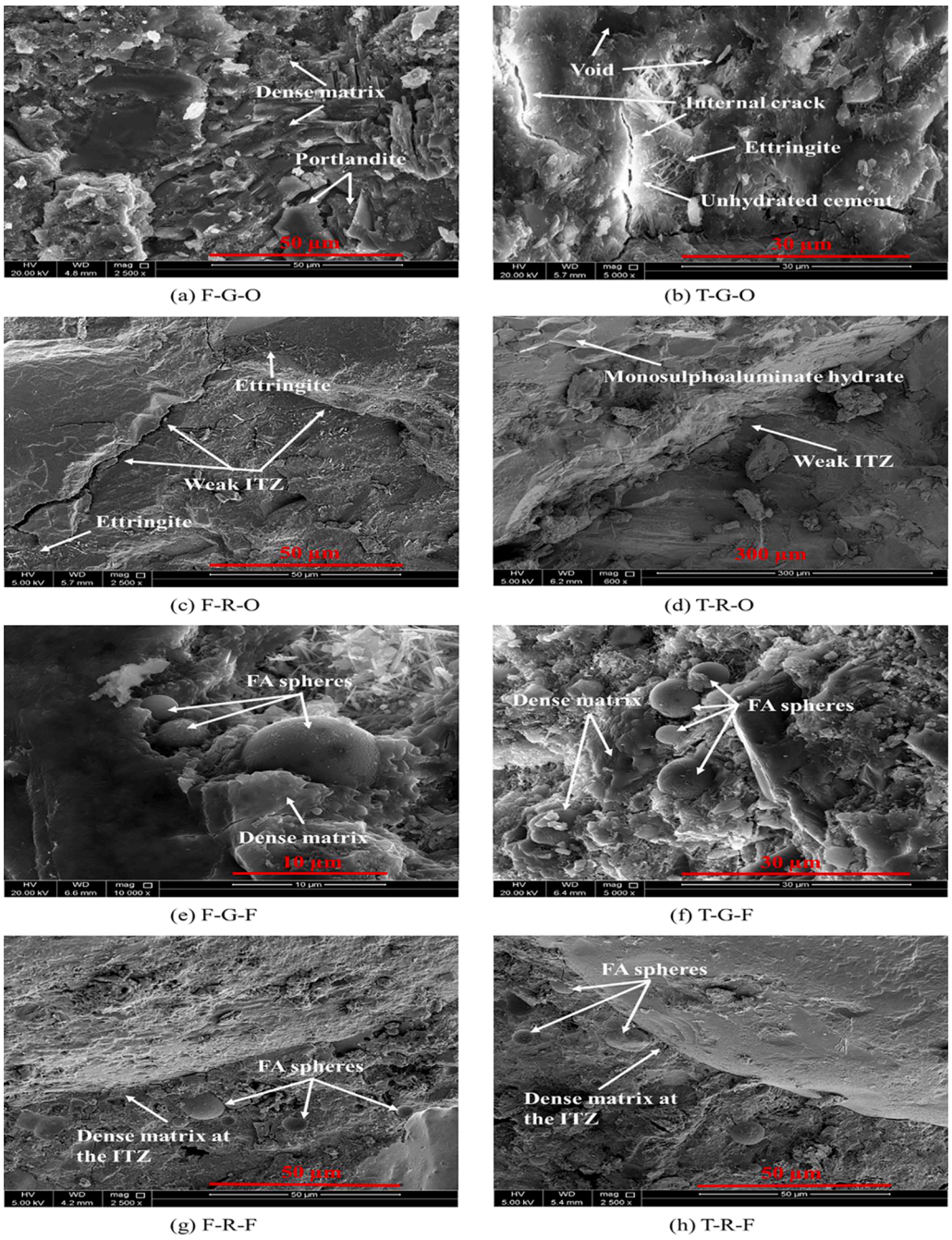

Fig. 11. SEM images of the concrete mixes.

RCA in specimen F-R-O increased the 28 and 90-day chloride permeability by 13.5% and 14.1% compared to specimen F-G-O (Fig. 10(b)), respectively. This increase was expected since FW-RAC specimens reported higher porosity than NAC. In addition, similar to porosity results, specimen T-R-O exhibited 32.1% and 14.6% lower chloride permeability than T-G-O and F-R-O at 28 days, respectively. As explained in Section 3.4.4, the formation of calcium monosulphoaluminate hydrate enhanced concrete micropores and decreased concrete pores. Moreover, in conformance with the porosity results, the reduction in the chloride permeability of RAC specimens after 90 days of curing was approximately similar to their counterparts with GA.

It could also be noticed that the incorporation of 20% FA greatly decreased concrete chloride permeability, regardless of mixing water and aggregate types (Fig. 10(c)). The Coulomb charges of specimens F-G-F, T-G-F, F-R-F, and T-R-F were decreased by 43.4%, 51.2%, 44.5%, and 40% at 28 days and 47.3%, 68.1%, 47.8%, and 50.4% at 90 days, respectively, compared to their counterparts without FA. This is attributed to the small-size spherical particles of FA and the C–S–H gel, which have effectively filled concrete pores and cracks. In addition, after curing for 90 days, FA concrete specimens recorded 31% to 42% enhancement in the chloride permeability, whilst other specimens without FA achieved enhancement of only 11% to 27%, signifying the influence of the pozzolanic reaction in improving the long-term durability of concrete. In this context, specimen T-R-F experienced the lowest chloride permeability at 90 days due to the formation of both monosulphoaluminate hydrate and C–S–H gel, which effectively improved the cohesion of the ITZ layers. The findings are in line with the experimental results of Ahmed et al. [4] and Ali et al. [19].

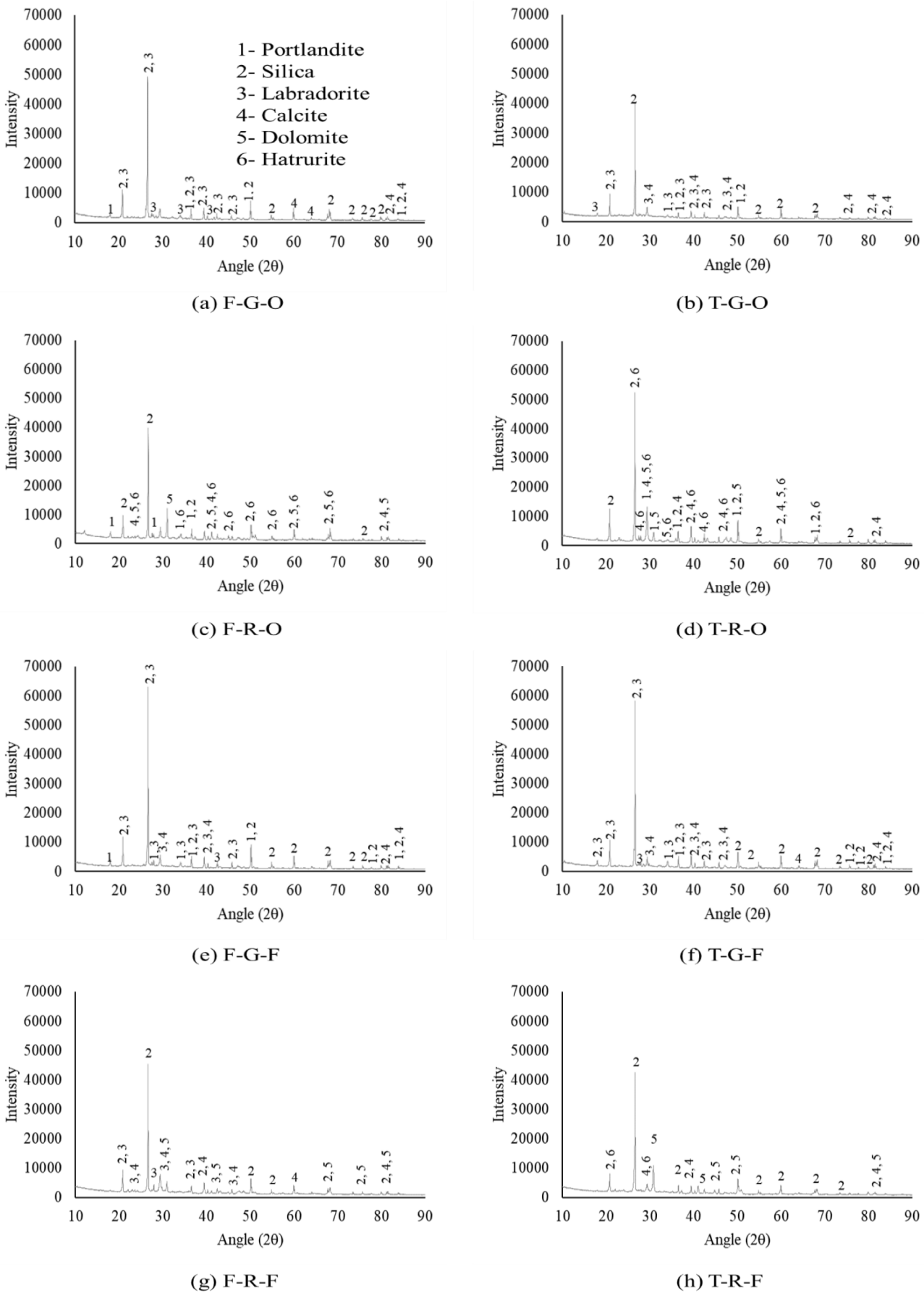

Fig. 12. XRD intensities of the concrete mixes.

3.5. Concrete microstructural and mineralogy analysis

It is well known that concrete pores and discontinuities significantly affect concrete mechanical and durability properties. Therefore, SEM images illustrating concrete microstructure were prepared and analyzed in this study. As shown in Fig. 11(a) and (b), mix F-G-O demonstrated denser microstructure and higher amounts of portlandite than mix T-G-O, whilst mix T-G-O exhibited considerable amounts of un-hydrated cement (shown in white color [1]), pores (shown in black color [1]), and internal-continuous cracks at different places due to the phosphate, zinc, and suspended solids in TWW, which delayed the OPC hydration process and weakened the ITZ layer between aggregates and cement matrix. This could explain why TWW concrete recorded lower strength and durability properties than FW concrete. Furthermore, Fig. 11(c) and (d) depicts that multiple weak ITZ layers existed between RCA and cement matrix in mixes F-R-O and T-R-O. These weak layers, in turn, promoted concrete internal cracks and voids and thus decreased the adhesive force between RCA and concrete matrix. As a result, RAC mixes recorded lower mechanical and durability properties than NAC mixes. In addition, the images reveal that mix F-R-O exhibited ettringite needles, owing to the high amounts of calcium in RCA, which accelerated the formation of ettringite needles. However, the ettringite needles were not presented in mix T-R-O because the calcium ions in RCA reacted with sulfate in TWW and generated calcium monosulphoaluminate hydrate. This explains why mix T-R-O achieved lower porosity and chloride permeability than mix F-R-O. Moreover, Fig. 11(e)–(h) shows that FA concrete mixes reported the most densified mixes because of the small-size spherical particles of FA and the C–S–H gel, which have effectively filled concrete pores that were induced by the suspended particles of TWW and the adhered mortar of RCA and thus enhanced the weak ITZ layers. As a result, the mix made with TWW, RCA, and 20% FA (T-R-F) reported significantly better durability properties as compared with those made completely with OPC.

By observing concrete XRD intensities in Fig. 12, it was noticed that mix T-G-O had slightly lower intensities of portlandite and labradorite than mix F-G-O (Fig. 12(a) and (b)). The lower intensities of portlandite and labradorite and the presence of un-hydrated cement particles in TWW concrete support the formation of Ca-phosphate and $CaZn_2(OH)_6{\cdot}2H_2O$, which caused a reduction in the hydration of OPC and consequently decreased the compressive and flexural strength of concrete. Furthermore, it was observed that RAC mixes F-R-O and T-R-O are composed of dolomite ($CaMg(CO_3)$), resulting from parent concrete's impurities (Fig. 12(c) and (d)). The presence of calcium ions in the dolomite without a sufficient amount of C–S–H hydrate accelerate the formation of ettringite needles ($C_6AS_3H_{32}$), and hence more voids are formed in concrete. This phenomenon combined with the porous nature of RCA is the main reasons behind the significant drop in the performance of RAC mixes. Meanwhile, complying with the experimental results, Fig. 12(c) and (d) reveals that mix T-R-O noticeably reported a higher amount of hatrurite ($Ca_3(SiO_4)O$) than F-R-O, indicating more C–S–H hydrate for mix T-R-O. For that reason, mix T-R-O showed better properties than F-R-O. Moreover, Fig. 12(e)–(h) reveals that FA concrete mixes reported the highest amounts of silica and labradorites. This is due to the pozzolanic reaction between FA and $Ca(OH)_2$, which produced more C–S–H gel and consequently densified the cement matrix. In addition, a higher amount of hatrurite could be seen in mix T-R-F compared to other FA concrete mixes. The presence of hatrurite, silica, and labradorites explains why mix T-R-F exhibited the lowest chloride permeability among the investigated mixes.

4. Conclusions

In the current study, the mechanical and durability performance of concrete simultaneously made with TWW, RCA, and FA were evaluated. The mechanical tests included concrete slump, density, and compressive and flexural strengths, while the durability tests comprised of concrete resistivity, porosity, and chloride permeability. In addition, aggregate and concrete microstructural and mineralogy were studied to support the experimental results. Based on the results obtained, the following conclusions were made:.

1- The type of mixing water and coarse aggregates had little-to-no influence on the fresh properties of concrete. However, replacing 20% of OPC with FA significantly enhanced concrete slump.
2- TWW concrete recorded 6% to 12% lower compressive strength and 8% to 10% lower flexural strength than reference concrete. Moreover, FW-RAC mixes recorded up to 21% and 10% lower compressive and flexural strength than FW-NAC mixes, respectively. However, TWW-RAC mixes recorded higher flexural strength than TWW-NAG mixes. Furthermore, the incorporation of 20% FA decreased the compressive and flexural strength up to 34% and 14%, respectively.
3- The electrical resistivity was decreased by 5% to 7.5% when FW was replaced with TWW. In addition, replacing GA with RCA decreased the electrical resistivity by 6% to 15%.
4- Concrete porosity and chloride permeability were increased by 40% to 77% when FW was replaced with TWW. Moreover, FW-RAC mixes reported an average increase of 23% and 14% in porosity and chloride permeability compared to reference concrete, respectively. Furthermore, TWW-RAC mixes reported an average decrease of 4.6% and 12.6% in the porosity and chloride permeability, respectively, compared to FW-RAC mixes.
5- In contrast to the loss in the hardened mechanical properties of FA concrete mixes, all durability properties were greatly enhanced by 18% to 51% when 20% of OPC was replaced with FA.
6- Concrete made with TWW, RCA, and 20% FA exhibited the lowest chloride permeability among the investigated mixes.
7- Concrete microstructural analysis showed that RAC and TWW concrete mixes had more pores and discontinuities than reference concrete. Furthermore, FA showed the potential to fill the voids that are induced by RCA and TWW, and thus enhanced the ITZ layers and durability properties.

As a result, this study showed that TWW, RCA, and FA could be utilized as sustainable alternatives to traditional concrete raw materials. However, in order to improve the reliability and practicality of these materials, it is recommended that research on the chloride migration properties of TWW-RAC be conducted over a longer period of time.

CRediT authorship contribution statement

Abdelrahman Abushanab: Investigation, Formal analysis, Data curation, Software, Writing – original draft, Visualization. **Wael Alnahhal:** Conceptualization, Methodology, Validation, Writing – review & editing, Resources, Funding acquisition, Supervision, Project administration.

Declaration of Competing Interest

The authors declare that they have no known competing financial interests or personal relationships that could have appeared to influence the work reported in this paper.

Acknowledgments

This publication was made possible by GSRA grant GSRA6-1-0509-19022 from the Qatar National Research Fund (QNRF, a member of Qatar Foundation). The authors would like also to thank the Central Laboratories Unit (CLU) at Qatar University for the scanning electron microscopy images. Also, the financial support from Qatar University through grant no. QUST-1-CENG-2021-20 is acknowledged. The findings achieved herein are solely the responsibility of the authors.

References

[1] A. Abushanab, W. Alnahhal, Combined effects of treated domestic wastewater, fly ash, and calcium nitrite toward concrete sustainability, J. Build. Eng. 44 (2021) 103240, https://doi.org/10.1016/j.jobe.2021.103240.

[2] W. Alnahhal, O. Aljidda, Flexural behavior of basalt fiber reinforced concrete beams with recycled concrete coarse aggregates, Constr. Build. Mater. 169 (2018) 165–178, https://doi.org/10.1016/j.conbuildmat.2018.02.135.

[3] M.G. Sohail, W. Alnahhal, A. Taha, K. Abdelaal, Sustainable alternative aggregates: Characterization and influence on mechanical behavior of basalt fiber reinforced concrete, Constr. Build. Mater. 255 (2020) 119365, https://doi.org/10.1016/j.conbuildmat.2020.119365.

[4] S. Ahmed, Y. Alhoubi, N. Elmesalami, S. Yehia, F. Abed, Effect of recycled aggregates and treated wastewater on concrete subjected to different exposure conditions, Constr. Build. Mater. 266 (2021) 120930, https://doi.org/10.1016/j.conbuildmat.2020.120930.

[5] A. Abushanab, W. Alnahhal, M.G. Sohail, N. Alnuaimi, R. Kahraman, N. Altayeh, Mechanical and durability properties of ultra-high performance steel FRC made with discarded materials, J. Build. Eng. 44 (2021) 103264, https://doi.org/10.1016/j.jobe.2021.103264.

[6] A.H. Noruzman, B. Muhammad, M. Ismail, Z. Abdul-Majid, Characteristics of treated effluents and their potential applications for producing concrete, J. Environ. Manage. 110 (2012) 27–32, https://doi.org/10.1016/j.jenvman.2012.05.019.

[7] G. Asadollahfardi, M. Delnavaz, V. Rashnoiee, N. Ghonabadi, Use of treated domestic wastewater before chlorination to produce and cure concrete, Constr. Build. Mater. 105 (2016) 253–261, https://doi.org/10.1016/j.conbuildmat.2015.12.039.

[8] M.F. Arooj, F. Haseeb, A.I. Butt, D.M. Irfan-Ul-Hassan, H. Batool, S. Kibria, Z. Javed, H. Nawaz, S. Asif, A sustainable approach to reuse of treated domestic wastewater in construction incorporating admixtures, J. Build. Eng. 33 (2021) 101616, https://doi.org/10.1016/j.jobe.2020.101616.

[9] M. Shekarchi, M. Yazdian, N. Mehrdadi, Use of biologically treated domestic waste water in concrete, Kuwait J. Sci. Eng. 39 (2012) 97–111.

[10] A. Abushanab, W. Alnahhal, Characteristics of Concrete Made with Treated Domestic Wastewater, in: T. Kang, Y. Lee (Eds.), Springer Singapore, Singapore, 2022: pp. 231–235. https://doi.org/10.1007/978-981-16-6932-3_20.

[11] M.S. Hassani, G. Asadollahfardi, S.F. Saghravani, S. Jafari, F.S. Peighambarzadeh, The difference in chloride ion diffusion coefficient of concrete made with drinking water and wastewater, Constr. Build. Mater. 231 (2020) 117182, https://doi.org/10.1016/j.conbuildmat.2019.117182.

[12] S. Saxena, A.R. Tembhurkar, Impact of use of steel slag as coarse aggregate and wastewater on fresh and hardened properties of concrete, Constr. Build. Mater. 165 (2018) 126–137, https://doi.org/10.1016/j.conbuildmat.2018.01.030.

[13] S.B. Huda, M. Shahria Alam, Mechanical and Freeze-Thaw Durability Properties of Recycled Aggregate Concrete Made with Recycled Coarse Aggregate, J. Mater. Civ. Eng. 27 (10) (2015) 04015003, https://doi.org/10.1061/(ASCE)MT.1943-5533.0001237.

[14] Y. Wang, P. Hughes, H. Niu, Y. Fan, A new method to improve the properties of recycled aggregate concrete: Composite addition of basalt fiber and nano-silica, J. Clean. Prod. 236 (2019) 117602, https://doi.org/10.1016/j.jclepro.2019.07.077.

[15] G. Andreu, E. Miren, Experimental analysis of properties of high performance recycled aggregate concrete, Constr. Build. Mater. 52 (2014) 227–235, https://doi.org/10.1016/j.conbuildmat.2013.11.054.

[16] G. Dimitriou, P. Savva, M.F. Petrou, Enhancing mechanical and durability properties of recycled aggregate concrete, Constr. Build. Mater. 158 (2018) 228–235, https://doi.org/10.1016/j.conbuildmat.2017.09.137.

[17] N.A. Abdulla, Effect of Recycled Coarse Aggregate Type on Concrete, J. Mater. Civ. Eng. 27 (10) (2015) 04014273, https://doi.org/10.1061/(ASCE)MT.1943-5533.0001247.

[18] J. de Brito, J. Ferreira, J. Pacheco, D. Soares, M. Guerreiro, Structural, material, mechanical and durability properties and behaviour of recycled aggregates concrete, J. Build. Eng. 6 (2016) 1–16, https://doi.org/10.1016/j.jobe.2016.02.003.

[19] B. Ali, L.A. Qureshi, S.H.A. Shah, S.U. Rehman, I. Hussain, M. Iqbal, A step towards durable, ductile and sustainable concrete: Simultaneous incorporation of recycled aggregates, glass fiber and fly ash, Constr. Build. Mater. 251 (2020) 118980, https://doi.org/10.1016/j.conbuildmat.2020.118980.

[20] M. Alhawat, A. Ashour, Bond strength between corroded steel and recycled aggregate concrete incorporating nano silica, Constr. Build. Mater. 237 (2020) 117441, https://doi.org/10.1016/j.conbuildmat.2019.117441.

[21] T. Cheewaket, C. Jaturapitakkul, W. Chalee, Long term performance of chloride binding capacity in fly ash concrete in a marine environment, Constr. Build. Mater. 24 (8) (2010) 1352–1357, https://doi.org/10.1016/j.conbuildmat.2009.12.039.

[22] C. Lima, A. Caggiano, C. Faella, E. Martinelli, M. Pepe, R. Realfonzo, Physical properties and mechanical behaviour of concrete made with recycled aggregates and fly ash, Constr. Build. Mater. 47 (2013) 547–559, https://doi.org/10.1016/j.conbuildmat.2013.04.051.

[23] R. Kurda, J. de Brito, J.D. Silvestre, Influence of recycled aggregates and high contents of fly ash on concrete fresh properties, Cem. Concr. Compos. 84 (2017) 198–213, https://doi.org/10.1016/j.cemconcomp.2017.09.009.

[24] S.C. Kou, C.S. Poon, D. Chan, Influence of fly ash as a cement addition on the hardened properties of recycled aggregate concrete, Mater. Struct. 41 (7) (2008) 1191–1201, https://doi.org/10.1617/s11527-007-9317-y.

[25] World Health Organization, Guidelines for drinking-water quality, Geneva, Switzerland, 2011.

[26] ASTM 1602/C1602M − 18, Standard Specification for Mixing Water Used in the Production of Hydraulic Cement Concrete, 2018. https://doi.org/10.1520/C1602_C1602M-18.

[27] P.A. Wedding, B.D. Wheeler, Chemical Analysis of Portland Cement by Energy Dispersive X-Ray Fluorescence, Cem. Concr. Aggr. 5 (2) (1983) 123, https://doi.org/10.1520/CCA10262J.

[28] ASTM C150/C150M − 20, Standard Specification for Portland Cement, 2020. https://doi.org/10.1520/C0150_C0150M-20.

[29] ASTM C618 − 19, Standard Specification for Coal Fly Ash and Raw or Calcined Natural Pozzolan for Use in Concrete, 2019. https://doi.org/10.1520/C0618-19.

[30] M.& Eddy, M. Abu-Orf, G. Bowden, F.L. Burton, W. Pfrang, H.D. Stensel, G. Tchobanoglous, R. Tsuchihashi, A. (Firm), Wastewater engineering: treatment and resource recovery, McGraw Hill Education, 2014.

[31] ASTM C127-15, Standard Test Method for Relative Density (Specific Gravity) and Absorption of Coarse Aggregate, 2015. https://doi.org/10.1520/C0127-15.

[32] ASTM C131/C131M − 20, Standard Test Method for Resistance to Degradation of Small-Size Coarse Aggregate by Abrasion and Impact in the Los Angeles Machine, 2020. https://doi.org/10.1520/C0131_C0131M-20.

[33] BSI, BS 812-103.1:1985, Testing aggregates - Method for determination of particle size distribution - Sieve tests, BSI Standards Limited, 1998. https://doi.org/10.3403/00139627.

[34] ASTM C88/C88M–18, Standard Test Method for Soundness of Aggregates by Use of Sodium Sulfate or Magnesium Sulfate, (n.d.). https://doi.org/10.1520/C0088_C0088M-18.

[35] ASTM C33/C33M − 18, Standard Specification for Concrete Aggregates, 2018. https://doi.org/10.1520/C0033_C0033M-18.

[36] Standard Test Method for Slump of Hydraulic-Cement Concrete, ASTM C143/C143M-15a. (2015) 15–18. https://doi.org/10.1520/C0143_C0143M-15A.

[37] ASTM C138/C138M − 17a, Standard Test Method for Density (Unit Weight), Yield, and Air Content (Gravimetric) of Concrete, 2017. https://doi.org/10.1520/C0138_C0138M-17A.

[38] Standard Test Method for Compressive Strength of Cylindrical Concrete Specimens, ASTM C39/C39M-20. (2020) 1–8. https://doi.org/10.1520/C0039_C0039M-20.

[39] ASTM C78/C78M − 18, Standard Test Method for Flexural Strength of Concrete (Using Simple Beam with Third-Point Loading), 2018. https://doi.org/10.1520/C0078_C0078M-18.

[40] AASHTO TP 95, Standard Method of Test for Surface Resistivity Indication of Concrete's Ability to Resist Chloride Ion Penetration, American Association of State Highway and Transportation Officials, Washington, DC, 2011.

[41] ASTM C1754/C1754M-12, Standard Test Method for Density and Void Content of Hardened Pervious Concrete, 2012.

[42] ASTM C1202-19, Standard Test Method for Electrical Indication of Concrete's Ability to Resist Chloride Ion Penetration1, (2019). https://doi.org/10.1520/C1202-19.

[43] ASTM C1723 − 16, Standard Guide for Examination of Hardened Concrete Using Scanning ElectronSuns Microscopy, 2016. https://doi.org/10.1520/C1723-16.

[44] QCS, Qatar General Organization for Standards and Metrology, Qatar, 2014.

[45] H. Tan, F. Zou, M. Liu, B. Ma, Y. Guo, S. Jian, Effect of the Adsorbing Behavior of Phosphate Retarders on Hydration of Cement Paste, J. Mater. Civ. Eng. 29 (9) (2017) 04017088, https://doi.org/10.1061/(ASCE)MT.1943-5533.0001929.

[46] P. Siler, I. Kolarova, J. Bednarek, M. Janca, J. Masilko, R. Novotny, T. Opravil, The effect of zinc, water to binder ratio and silica fume on the hydration and mechanical properties of Portland cement mixtures, IOP Conf. Ser. Mater. Sci. Eng., IOP Publishing 583 (1) (2019) 012008, https://doi.org/10.1088/1757-899X/583/1/012008.

[47] K. Pimraksa, P. Chindaprasirt, 14 - Sulfoaluminate cement-based concrete, in: F. Pacheco-Torgal, R.E. Melchers, X. Shi, N. De Belie, K. Van Tittelboom, A.B.T.-E.-E. R. and R. of C.I. Sáez (Eds.), Woodhead Publ. Ser. Civ. Struct. Eng., Woodhead Publishing, 2018: pp. 355–385. https://doi.org/10.1016/B978-0-08-102181-1.00014-9.

[48] R. Kurad, J.D. Silvestre, J. de Brito, H. Ahmed, Effect of incorporation of high volume of recycled concrete aggregates and fly ash on the strength and global warming potential of concrete, J. Clean. Prod. 166 (2017) 485–502, https://doi.org/10.1016/j.jclepro.2017.07.236.